



A Journal of



## Accepted Article

**Title:** Synthesis of novel D- $\pi$ -A dyes for colorimetric cyanide sensing based on hemicyanine-functionalized N-(2-pyridyl)pyrazoles

**Authors:** Luz-Mery Garzón and Jaime Portilla

This manuscript has been accepted after peer review and appears as an Accepted Article online prior to editing, proofing, and formal publication of the final Version of Record (VoR). This work is currently citable by using the Digital Object Identifier (DOI) given below. The VoR will be published online in Early View as soon as possible and may be different to this Accepted Article as a result of editing. Readers should obtain the VoR from the journal website shown below when it is published to ensure accuracy of information. The authors are responsible for the content of this Accepted Article.

**To be cited as:** *Eur. J. Org. Chem.* 10.1002/ejoc.201901178

**Link to VoR:** <http://dx.doi.org/10.1002/ejoc.201901178>

Supported by



WILEY-VCH

# Synthesis of novel D- $\pi$ -A dyes for colorimetric cyanide sensing based on hemicyanine-functionalized *N*-(2-pyridyl)pyrazoles

Luz-Mery Garzón<sup>[a]</sup> and Jaime Portilla\*<sup>[a]</sup>

**Abstract:** Novel integrated *N*-(2-pyridyl)pyrazole-hemicyanine dyes (PH) were synthesized as promisor chemodosimeters for colorimetric and ratiometric CN<sup>-</sup> detection. These dyes, obtained by a three-step sequence starting from acetophenones in up to 69% overall yield, are donor- $\pi$ -acceptor (D- $\pi$ -A) systems consisting of indolium-salts bearing a modular donor aryl group on its pyrazole ring **PHa-e**. The salts displayed high selectivity and sensitivity for CN<sup>-</sup> (LOD of up to  $9.9 \times 10^{-7}$  M), as determined by interrupting the modular D- $\pi$ -A system by nucleophilic attack of the cyanide on its iminium group; the mechanism of this process was confirmed by Job's plot experiment, spectral analysis, cyclic voltammetry studies and TD-DFT calculations. This probe changes its color from deep yellow to colorless and can be used for in-the-field measurements without special equipment, since this change can be easily observed by the naked eye; indeed, yellow test strips were suitably used to detect CN<sup>-</sup> in water.

## Introduction

In recent years, studies on chemosensors based on optical responses have attracted the attention of researchers in the fields of chemistry, environmental science, biology, and engineering.<sup>[1]</sup> There are two general types of optical detection, a colorimetric detection where changes in color are produced that are visible to the naked eye and fluorimetric detection based on emission changes. A plethora of probes with diverse chromophores or fluorophores have been developed and used in the detection of different cations, anions, bioactive species, etc.<sup>[1,2]</sup> For example, the contamination of water by ionic species has a high environmental impact; one of the most toxic species is cyanide ion (CN<sup>-</sup>), whose salts have been used in the production of herbicides and fibers, the extraction of gold, the petrochemical industry and electroplating and metallurgy.<sup>[3]</sup>

Cyanide is extremely toxic to physiological systems and is mainly absorbed by skin and inhalation; indeed, in the bloodstream, it can inhibit the respiratory chain due to the formation of a stable complex leading to cytotoxic hypoxia and cellular asphyxiation.<sup>[4]</sup> The maximum permissible level of CN<sup>-</sup> in drinking water established by the World Health Organization (WHO) is  $19.0 \times 10^{-7}$  M;<sup>[5]</sup> thus, there are several methods for CN<sup>-</sup> sensing, such as electrochemistry, gas chromatography and the use of optical molecular sensors. These optical molecular sensors are chemosensors that have been widely studied as simple, selective and sensitive systems and consist of dyes formed by recognition and signaling units.<sup>[6]</sup> Among optical sensors, colorimetric probes are especially promising since the color change can be observed by the naked eyes, thus requiring less labour in measurements and not requiring any equipment.<sup>[7]</sup>

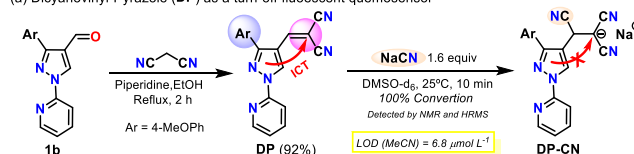
Some probes for anions can differentiate selectively between species with similar basicity and surface load density. There are diverse systems for CN<sup>-</sup> detection, based on the displacement of metals in complexes, aldehydes activated by hydrogen bonds and nucleophilic addition reactions, but some have drawbacks such as low selectivity and hydrophilicity and high detection limits (LOD).<sup>[8]</sup> Thus, research on methods for CN<sup>-</sup> sensing based on small molecules is highly desirable; in fact, our lab recently reported two new probes, pyrazole derivatives bearing conjugated dicyanovinylidene **DP**<sup>[9]</sup> or an indolium salt (hemicyanine moiety) **PpHe**<sup>[10]</sup> (Scheme 1). These donor-

$\pi$ -acceptor (D- $\pi$ -A) type dyes usually suffer from an intramolecular charge transfer (ICT) process with a ratiometric response that allows two points to follow-up and thus provides an integrated correlation for environmental interference.<sup>[9-11]</sup>

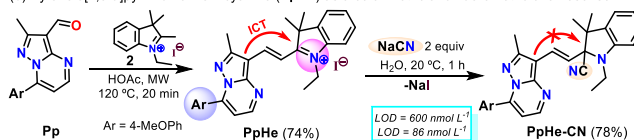
Detection of a specific analyte based on hemicyanines is generally achieved by adjusting the sensor molecule charge transfer process. It is possible to modulate the properties of this system type by changing the donor fragment,<sup>[9]</sup> and therefore, the optical response ( $\lambda_{ab}$ ,  $\lambda_{em}$ ) leads to colorimetric and ratiometric changes for a specific detection. However, some limitations of the hemicyanines should be overcome, such as unwanted aggregation in aqueous solution, Stokes shifts < 25 nm and poor photostability.<sup>[12]</sup> The D- $\pi$ -A organic dyes are important chemicals in elucidating the relations of push-pull chromophores with their optoelectronic properties,<sup>[13]</sup> which have been used in the design of fluorescent sensors,<sup>[14]</sup> dye-sensitized solar cells (DSSCs)<sup>[15]</sup> and organic light-emitting diodes (OLED).<sup>[16]</sup> Various heterocyclic cores, such as carbazole, coumarin, triazole, pyrazolo[1,5-*a*]pyrimidine and pyrazole, have been used as donor moieties in the construction of D- $\pi$ -A systems.<sup>[17]</sup> Among them, pyrazole derivatives have been proven to be good chromophores and show efficient electronic transfer. Consequently, pyrazoles have important photophysical properties, are used as optical whiteners in detergents, serve as UV stabilizers, and can be used in electrophotography and electroluminescence fields.<sup>[18]</sup>

### Our previous results

(a) Dicyanovinyl-Pyrazole (DP) as a turn-off fluorescent chemosensor<sup>[9]</sup>



(b) Pyrazolo[1,5-*a*]pyrimidine-Hemicyanine (PpHe) as a colorimetric and fluorometric chemosensor<sup>[10]</sup>



### This work

(c) Pyrazole-Hemicyanine dyes (PHa-e) as probes for CN<sup>-</sup> detection



**Scheme 1.** Synthesis of probes for cyanide detection based on the pyrazole derivatives **DP**, **PpHe** and **PH**.

[a] Departamento de Química, Universidad de los Andes, Carrera 1 N° 18A-12, Bogotá, Colombia

E-mail: [jportill@uniandes.edu.co](mailto:jportill@uniandes.edu.co)

<https://academia.uniandes.edu.co/AcademyCv/jportill>

† Supporting information (SI) for this article is available on the WWW under <http://dx.doi.org/>

## FULL PAPER

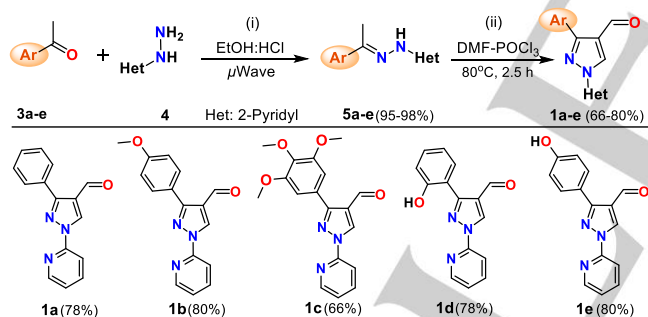
WILEY-VCH

Considering the aforementioned aspects together with our interest in developing efficient methods to prepare ion chemosensors,<sup>[9,10,19]</sup> we proposed the synthesis of novel hemicyanine-functionalized *N*-(2-pyridyl)pyrazoles **PHA-e** with a modular-donor aryl group at its pyrazole ring (Scheme 1c). In our previous works, formylpyrazole **1b** was used to obtain a **DP** probe that acts quickly since the 2-pyridyl group of the pyrazole ring favors its reactivity,<sup>[9,20]</sup> while the 3-formylpyrazolo[1,5-*a*]pyrimidine **Pp** reacted with indolium salt **2** to obtain **PpHe**, which acts more slowly.<sup>[10]</sup> The **PpHe** probe showed a lower LOD value than **DP**, probably because the structure of **PpHe** contains higher  $\pi$ -conjugation (Scheme 1a-b). Therefore, we expect that the new synthesized **PHA-e** probes have a shorter response time in  $\text{CN}^-$  sensing with than does **PpHe**, as well as lower LODs than **DP**, since **PHA-e** combine the best structural properties found in our previous works.<sup>[9,10]</sup>

## Results and discussion

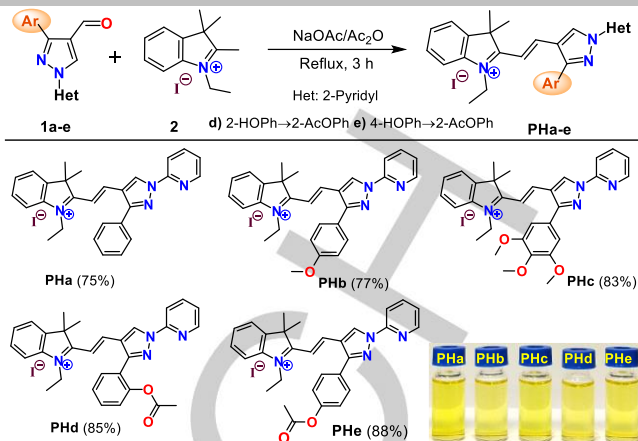
## Synthesis and characterization

The novel colorimetric probes **PHA-e** were successfully synthesized as orange-red solids (deep yellow in ethanolic solution, 75–88% yield) by the Knoevenagel reaction of the appropriate 4-formylpyrazole **1a-e** with indolium salt **2** (Scheme 3). In the complete synthetic route of **PHA-e** shown in Scheme S1 of the Supporting Information (SI†), we can observe that **PHA-e** were obtained via three reaction steps starting from acetophenones **3a-e** and 2-hydrazinylpyridine (**4**). The synthesis of precursors **1a-e** occurred in the first two steps (Scheme 2). The first step included a condensation reaction between **3a-e** and **4** to form hydrazones **5a-e** in high yields, followed by a Vilsmeier–Haack reaction (formylation-cyclization-formylation) to give the desired aldehydes in good yields. As a result, the novel hybrid compounds **PHA-e** were obtained in good overall yields (52–69%).



**Scheme 2.** Synthesis of 3-aryl-1-pyridin-2-yl-1H-pyrazole-4-carbaldehyde **1a-e**. Conditions: (i) **3a-e** (4.58 mmol) and **4** (4.58 mmol) in EtOH:HCl (5:1 v/v) under microwave irradiation at 95 °C for 10 min; (ii) **5a-e** (2.50 mmol) and  $\text{POCl}_3$ /DMF (12.5/7.5 mmol, 1.17/0.58 mL) in DMF (5 mL).

The structures of all synthesized compounds (**PHA-e**, **1a-e** and **5a-e**) were elucidated by NMR spectroscopy and HRMS analysis (Figs. S2–S22, SI†). TGA of the probes was carried out to verify their high thermal stability and low solvent residues (Fig. S1, SI†), which is important for subsequent photophysical studies. It should be noted that hydrazones **5a-e** were obtained through microwave (MW) irradiation with higher yields, shorter reaction times and easier purification processes than in our previous work.<sup>[9]</sup> Furthermore, in the case of compounds **PHd-e**, acetylation of the OH group in their respective precursors also occurred, while the Knoevenagel reaction did not occur under conditions similar to those used in our other previous work (MW in acetic acid)<sup>[10]</sup> (Schemes 1 and 3).



**Scheme 3.** Synthesis of the colorimetric probes **PHA-e** from 4-formylpyrazoles **1a-e**. Conditions: 4-formylpyrazole **1a-e** (0.50 mmol), indolium salt **2** (0.65 mmol) and NaOAc (0.65 mmol) in 2.0 mL of acetic anhydride. [a] Photograph of **PHA-e** dissolved in ethanol ( $4.0 \times 10^{-5}$  M) under natural light.

## Photophysical and sensing properties

UV–vis and fluorescence spectra of **PHd-e** were obtained in toluene (PhMe), dichloromethane (DCM), acetonitrile (ACN), dimethyl sulfoxide (DMSO), ethanol (EtOH) and water ( $\text{H}_2\text{O}$ ) at  $1.0 \times 10^{-5}$  M (Figs. S23–S27 and Table S1, SI†). The UV–Vis spectra of **PHA-e** show two absorption bands, one at approximately 300 nm attributed to  $\pi \rightarrow \pi^*$  transitions and the other in the range of 400 to 450 nm attributed to  $\text{So} \rightarrow \text{ICT}$  transitions caused by an ICT from the pyrroly-type N atom of the pyrazole ring to the  $\text{C}=\text{N}^+$  group (Scheme 1c). Thus, the absorption spectra of compounds **PHA-e** are largely influenced by the polarity of the microenvironment, and in this case, a hypsochromic shift is observed as the polarity of the solvent increases. These findings are explained by the ionic nature of the salts **PHA-e**, which have greater dipole moments in the ground state than in the excited state, and upon excitation, the molecular dipole weakens and reorients.<sup>[12,21]</sup> As expected, the ICT bands of **PHA-e** were bathochromically shifted by increasing the donor nature of the aryl group (i.e., 2-OAc < 4-OAc < H < 3,4,5-(MeO)<sub>3</sub> < 4-MeO).<sup>[17,22]</sup>

Regarding the fluorescence experiments of **PHA-e**, the results were not significant in any of the evaluated solvents, as all compounds showed low quantum yields (Table S1, SI†), possibly due to the formation of nonfluorescent aggregates.<sup>[23]</sup> Notably, decreasing the donor nature of the aryl group of the pyrazole ring results in a greater Stokes shift (Table S1, SI†). It is possible that the ICT phenomenon in **PHd** (pyrazole  $\rightarrow \text{C}=\text{N}^+$ ) is better than that in **PHa** ( $\text{Ar} \rightarrow \text{C}=\text{N}^+$ ). Considering the revealed photophysical properties of these D– $\pi$ –A systems, we decided to study the potential use of these materials in the design of colorimetric chemosensors for anion detection. These salts have moderate solubility in water; thus, an EtOH:H<sub>2</sub>O (1:1) mixture (easily accessible and easy to handle) was selected for later studies. This study was carried out because **PHA-e** possesses a hemicyanine electrophilic group **H** conjugated with a donor pyrazole moiety **Pa-e**. Accordingly, the addition of a suitable nucleophile could interrupt the ICT between these two structural moieties **Pa-e**  $\rightarrow$  **H**, leading to the loss of its absorption properties.<sup>[10,23]</sup>

To evaluate the use of **PHA-e** salts in anion sensing, UV-vis absorption spectra of **PHA-e** ( $4.0 \times 10^{-5}$  M in ethanol) were measured after 10 min of reaction at room temperature with 3 equiv of  $\text{CN}^-$  or other anions ( $\text{OAc}^-$ ,  $\text{Br}^-$ ,  $\text{HSO}_4^-$ ,  $\text{NO}_3^-$ ,  $\text{ClO}_3^-$ ,  $\text{F}^-$ ,  $\text{H}_2\text{PO}_4^-$ ,  $\text{I}^-$ ,  $\text{N}_3^-$ ,  $\text{NO}_2^-$ ,  $\text{S}_2^-$ ,  $\text{SCN}^-$ ,  $\text{SO}_4^{2-}$ ) dissolved in water, achieving EtOH:H<sub>2</sub>O (1:1 v/v) final solutions. No significant change in the absorption band was observed for any of the anions tested except for  $\text{CN}^-$ , with the disappearance of the ICT band (approximately 420 nm) and an increase in the intensity at approximately 300 nm (Figs. S28–S32, SI†). Consequently, the designed molecules are colorimetric and ratiometric probes of  $\text{CN}^-$ ,

## FULL PAPER

WILEY-VCH

where nucleophilic addition of this anion to the C=N<sup>+</sup> moiety blocks formation of these D-π-A systems, which is accompanied by important photophysical changes and a fast color change (deep yellow to colorless) that is visible to the naked eye (Fig. 1). It is important to note that **PHe** exhibited lower selectivity than **PHa-d** (Figs. S28–S32, S1†). It is possible that the ICT process in **PHe** (Ar→C=N<sup>+</sup>) is weakened by the acetyl group effect, while in **PHa-d**, there are electronic and conformational phenomena that favor this process (Fig. S46, S1†).

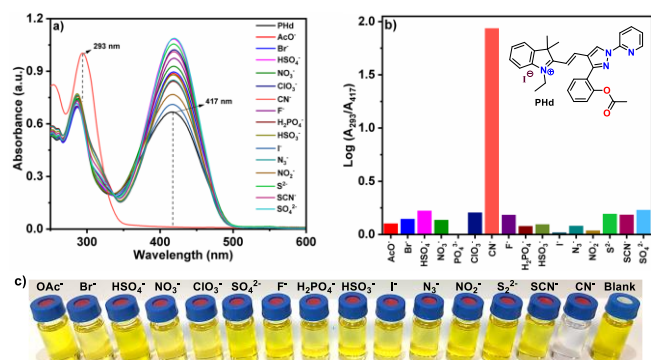


**Figure 1.** (a) Absorption spectra of **PHd** ( $4.0 \times 10^{-5}$  M) with  $\text{CN}^-$  and different anions (3 equiv,  $1.2 \times 10^{-4}$  M) in EtOH:H<sub>2</sub>O (1:1). (b)  $\text{Log}(A_{293}/A_{417})$  of **PHd** in the presence of 3 equiv of different anions. (c) Photograph of color changes under natural light with 3 equiv of the respective anion.

Probes **PHb** and **PHd** exhibited the highest selectivity towards  $\text{CN}^-$  (Figs. 1, S29 and S31); thus, we further studied the reaction using these salts ( $4.0 \times 10^{-5}$  M in ethanol) to determine the needed amount of  $\text{CN}^-$  to achieve total disappearance of the ICT band. UV-vis spectra were recorder after 1 min of reaction, and an excellent linear relationship ( $R^2_{\text{PHb}} = 0.999$  and  $R^2_{\text{PHd}} = 0.996$ ) was observed between  $\text{Log}(A_1/A_2)$  and the  $\text{CN}^-$  ion concentration after progressive addition of this anion (0.1 to 1.0 equiv) to salt solutions (Figs. 2 and S33–S34). From this linearity, the limit of detection for each probe was determined using the formula  $\text{LOD} = 3\sigma/k$ , where  $\sigma$  is the standard deviation from 10 measurements and  $k$  is the slope of the line. The LOD of an analytical method is the lowest amount of analyte in a sample that can be detected but not necessarily quantitated as an exact value.<sup>[24]</sup> The results indicate that  $\text{LOD}_{\text{PHb}} = 11.5 \times 10^{-7}$  M and  $\text{LOD}_{\text{PHd}} = 9.9 \times 10^{-7}$  M are well below  $19.0 \times 10^{-7}$  M, which is the maximum concentration permitted for drinking water by the WHO.<sup>[5]</sup>

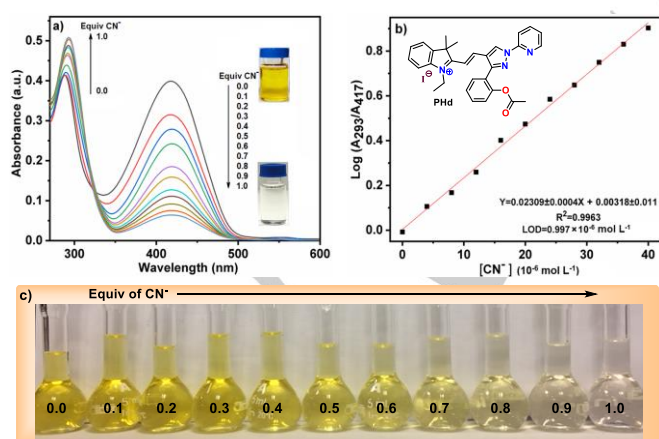


**Figure 2.** (a) UV-Vis absorption titration spectra of **PHd** ( $4.0 \times 10^{-5}$  M) in the presence of  $\text{CN}^-$  (0–1 equiv) in EtOH:H<sub>2</sub>O (1:1). (b) Linear relationship of  $\text{Log}(A_{293}/A_{417})$  versus  $[\text{CN}^-]$ . (c) Photograph of color changes (by titration) under natural light.

Additional studies were performed using the chemodosimeter **PHd** to better understand the response of this probe type to cyanide ions (Figs. 3 and S35). For instance, we investigated the time influence of time on the sensing system results by plotting the absorption intensity

versus reaction time, finding strong changes after 5 min and an equilibrium at nearly 10 min (Fig. 3a). Likewise, the selectivity of **PHd** towards  $\text{CN}^-$  at various pH values (from 2 to 11) was explored, with good cyanide recognition achieved in a pH range of 7–9 in phosphate buffer solutions (Fig. 3b). Finally, Job's plot method (absorbance) was used to determine the recognition stoichiometry using the reaction of **PHd** with cyanide ions.<sup>[25]</sup> The curve obtained in this experiment showed a maximum at approximately 0.5, suggesting a stoichiometric ratio **PHd**: $\text{CN}^-$  of 1:1 (Fig. S35).

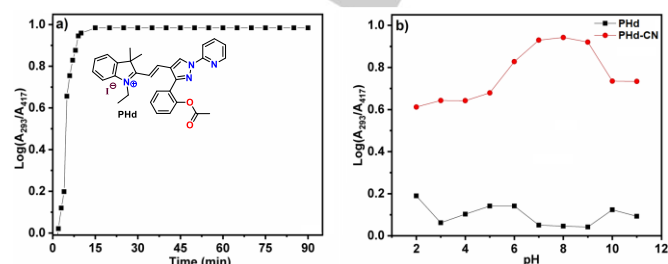


**Figure 3.** (a) Time-dependent absorption intensity ratio for **PHd** upon addition of 1.0 equiv of  $\text{CN}^-$  ( $4.0 \times 10^{-5}$  M in EtOH:H<sub>2</sub>O, 1:1). (b) Absorption intensity ratio of **PHd** ( $4.0 \times 10^{-5}$  M) and **PHd-CN** ( $4.0 \times 10^{-5}$  M each) as a function of pH in EtOH:H<sub>2</sub>O (1:1).

On the other hand, since the designed colorimetric probes rapidly change their color from deep yellow to colorless and this change can be easily detected by the naked eye, we conducted a preliminary study to achieve quantitative measurements of  $\text{CN}^-$  without special equipment. Thus, yellow test strips of chemodosimeter **PHd** were prepared by immersing white filter paper into an ethanolic solution ( $1.2 \times 10^{-4}$  M) and drying in an oven at 40 °C for 20 min. Then, the test strips were dipped into aqueous solutions of  $\text{CN}^-$  with varying concentrations (0.00, 0.25, 0.50, 0.75, and 1.00 equiv), and obvious color changes from deep yellow to white were observed (Fig. 4a). To further confirm the practical applicability of **PHd** for  $\text{CN}^-$  detection, qualitative studies of both selective and competition were carried out using 3 equiv of interfering anions (Fig. 4b). Only the addition of  $\text{CN}^-$  can lead to important color changes, but the other tested anions did not exhibit any influence. These results confirmed that **PHd** has higher selectivity towards  $\text{CN}^-$  than towards the other tested anions.

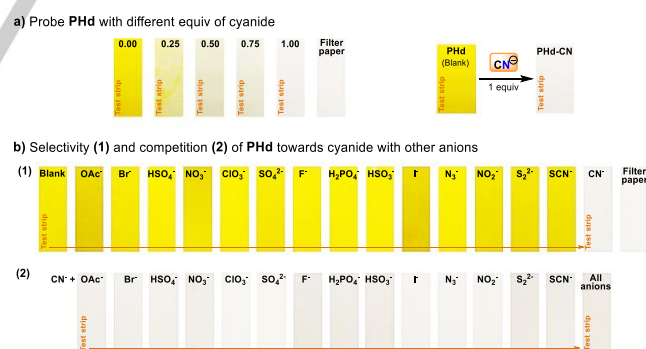


**Figure 4.** (a) Detection of  $\text{CN}^-$  in water at different concentrations using yellow test strips of **PHd** ( $1.2 \times 10^{-4}$  M). (b) Selectivity (1) and competition (2) of **PHd** towards  $\text{CN}^-$  (1 equiv) with other anions (3 equiv) using yellow-test strips of **PHd**.

## Frontier molecular orbital studies

Cyclic voltammetry (CV) was employed to study the electrochemical properties of the probes **PHa-e** and of the addition product **PHb-CN** and hence to estimate their HOMO (highest occupied molecular orbital) and LUMO (lowest unoccupied molecular orbital) energy levels. This study was carried out at room temperature using solutions of each compound in acetonitrile ( $10^{-4}$  M) with TBAPF<sub>6</sub> (0.1 M) as the supporting electrolyte. Oxidation and reduction potentials were measured against a Ag/AgCl reference electrode using ITO as the working electrode and a platinum wire as the counter electrode. The

## FULL PAPER

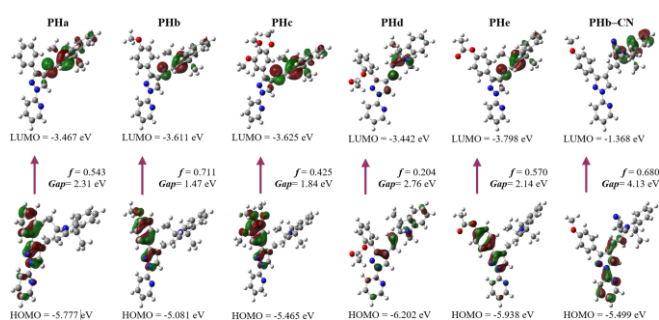
WILEY-VCH

one-electron oxidation of  $\text{PH}^{\text{x}}$  generates the resultant  $\text{PH}^{\text{x}+2}$ .<sup>[26]</sup> The voltammograms of  $\text{PHA-e}$  show irreversible oxidation-reduction processes possibly due to rapid dimerization (radical-radical coupling) of the corresponding radical dications (Fig. S40–S44, S1<sup>†</sup>),<sup>[23,27]</sup> while for  $\text{PHb-CN}$  a reversible process is shown (Fig. S45, S1<sup>†</sup>).

The introduction of donor groups in the pyrazole moiety results in a decrease in the oxidation potential (Table S2, S1<sup>†</sup>), and on the basis of the determined oxidation potential, the HOMO energy was estimated using the formula  $\text{HOMO} = -(E_{\text{ox}}^{\text{PHA-e}} + 4.8\text{eV} - E_{\text{ox}}^{\text{F}})$ ,<sup>[28]</sup> with ferrocene (F) as an external standard (Fig. S38, S1<sup>†</sup>). Subsequently, the bandgap<sup>[29]</sup> was estimated with the UV–Vis spectra, and with this value, the LUMO energy was estimated using the formula  $\text{LUMO} = \text{HOMO} + E_{\text{g}}$  (Table S2). As expected, the results show that probes substituted with the most donor groups have lower energy HOMO and smaller bandgaps than the other probes. Additionally, the frontier orbital energy levels of these D– $\pi$ –A systems are suitable for hole and electron injection, such as in push-pull chromophores with optoelectronic activity.<sup>[13]</sup>

To gain deeper insight into the electronic properties of the six studied compounds  $\text{PHA-e}$  and  $\text{PHb-CN}$ , time-dependent density functional theory (TDFT) calculations were performed in acetonitrile. The  $\lambda_{\text{max}}$  values were obtained from the theoretical UV–vis spectra with a theory level of B3LYP/6-31G (d,p). The maximum calculated UV absorptions, the theoretical electronic excitation energies, the calculated oscillator forces and the electronic gas phase transitions are detailed in Table S3 of the S1<sup>†</sup>. The band at approximately 420 nm is assigned mainly to HOMO-1→LUMO transitions in  $\text{PHA}$ , HOMO-2→LUMO in  $\text{PHb}$ , HOMO-3→LUMO in  $\text{PHc}$ , HOMO-1→LUMO transitions in  $\text{PHd}$ , and HOMO-1→LUMO transitions in  $\text{PHe}$ , indicating that these are So→ICT in nature.

According to the diagrams of frontier orbitals of these transitions (Fig. S46, S1<sup>†</sup>), it can be observed how the electronic nature of the aryl groups has a great influence on the ICT towards the  $\text{C}=\text{N}^+$ , except for  $\text{PHd}$ , where the transfer occurs from the pyrrole-type N atom of the pyrazole ring. It is possible that the steric effect that occurs between the pyridine-type N atom of the pyrazole (free electron pair) and the acetyl group of  $\text{PHd}$  is responsible for this fact, since its molecular conformation prevents  $\pi$  conjugation from the acetyl towards the  $\text{C}=\text{N}^+$ . The theoretical results corroborate the trend of  $\text{PHd} < \text{PHe} < \text{PHA} < \text{PHc} < \text{PHb}$  for the energy value of the HOMO estimated by CV and in turn the value of the bandgap ( $\Delta E$ ) in the synthesized probes (Scheme 4 and Table S3 of S1<sup>†</sup>).



Scheme 4. Estimation of HOMO and LUMO of compounds  $\text{PHA-e}$  and  $\text{PHb-CN}$ .

#### Proposed sensing mechanism for $\text{CN}^-$

Based on the results obtained, we have more deeply studied and verified the  $\text{CN}^-$  sensing mechanism *via* MS analysis and  $^1\text{H}$  NMR experiments of the product  $\text{PHb-CN}$  (easier  $^1\text{H}$  NMR spectra). The electrospray ionization mass spectrum (MS-ESI) confirmed the formation of the expected product (Fig. S38). The ion peak at  $m/z$  476.25 (intensity of 10%) corresponds to the product obtained by  $\text{CN}^-$  addition to the  $\text{C}=\text{N}^+$  moiety of  $\text{PHb}$  [ $\text{PHb-CN}$ ] $\text{H}^+$  (calcd, 476.24). The  $^1\text{H}$  NMR spectrum confirms the regioselectivity of the  $\text{CN}^-$  addition reaction (Fig. S37, S1<sup>†</sup>), since the aromatic protons and the methylene

group in  $\text{PHb}$  experienced important changes upon addition of the anion. In addition, the protons of the geminal methyl groups show the incorporation of  $\text{CN}^-$  in the  $\text{C}=\text{N}^+$  because in  $\text{PHb-CN}$ , these groups are not equivalent, while in  $\text{CN-PHb}$ , they are equivalent. In addition, no signal for the methino proton ( $\text{H}^*$ ) was observed at low field,<sup>[10]</sup> which confirms the formation of  $\text{PHb-CN}$  (Scheme 5 and Figs. S36–S37 in the S1<sup>†</sup>).



Scheme 5. Selectivity of the  $\text{CN}^-$  addition over  $\text{PHb}$  and proposed sensing mechanism.

This mechanism is consistent with all the results obtained herein and those previously reported by us,<sup>[8d,9,10]</sup> since the addition of  $\text{CN}^-$  to  $\text{PHA-e}$  blocks formation of the D– $\pi$ –A system together with the ICT process, which leads to important photophysical changes. In addition, this mechanism explains the competition with respect to other nucleophilic anions and why some probes (*i.e.*,  $\text{PHA}$ ,  $\text{PHc}$  and  $\text{PHe}$ ) were less selective. It is possible that the 2-pyridyl group of the pyrazole ring and certain arylc substitutions in this heterocycle make the  $\text{C}=\text{N}^+$  more electrophilic and selective. As shown in the molecular orbital diagram (Scheme 4), it is probable that  $\text{PHd}$  is more selective because its charge density is lower (the better reactivity) than those of the other probes because of the steric effect on its aryl group (2-OAcPh), which induces a conformation that blocks  $\pi$ -conjugation; while the high selectivity of  $\text{PHb}$  is due to the best donor effect (the better ICT process) of its 3-aryl group (4-MeOPh).

## Conclusions

In summary, novel D– $\pi$ –A chemodosimeters  $\text{PHA-e}$  for cyanide ion detection based on hybrid pyrazole–hemicyanine systems have been synthesized by a three-step sequence in up to 69% overall yield. These probes have a modular donor aryl group at the pyrazolic ring that promotes high selectivity and sensitivity towards  $\text{CN}^-$  versus other anions with LODs as low as  $9.9 \times 10^{-7}$  M, which is crucial for studies in aqueous samples.<sup>[5]</sup> The sensing mechanism (verified by MS and NMR) consists of the regioselective  $\text{CN}^-$  addition to the  $\text{C}=\text{N}^+$  moiety of the probes yielding products  $\text{PH-CN}$ , resulting in an increase in the  $\pi \rightarrow \pi^*$  band and a decrease in the So→ICT band with a ratiometric response. Moreover, CV experiments and TD-DFT calculations established that the selectivity and sensitivity of the probes depends on the type of substituent in the donor moiety and that there was an ICT obstruction in  $\text{PH-CN}$ . Thus,  $\text{PHA-e}$  appear to be good models for the development of simple and practical colorimetric probes for in-field measurements without special equipment.

## Experimental Section

### General

All reagents were purchased from commercial sources and used without further purification. The reactions were monitored by thin-layer chromatography (TLC) and visualized by a UV lamp (254 or 365 nm). Column flash chromatography was performed on silica gel (230–400 mesh). Microwave (MW) irradiation of the reactions was performed using a sealed reaction vessel (10.0 mL, max pressure = 300 psi) containing a Teflon-coated stir bar (obtained

from CEM) and a CEM Discover™ focused MW reactor ( $\nu = 2.45$  GHz) equipped with a built-in pressure measurement sensor and a vertically focused IR temperature sensor. Controlled temperature, power, and time settings were used for all reactions. The NMR spectra were recorded on a Bruker Avance 400 (400.13 MHz for  $^1\text{H}$ ; 100.61 MHz for  $^{13}\text{C}$ ) at 298 K. The NMR spectroscopic data were recorded in  $\text{CDCl}_3$  with the residual non-deuterated signal for  $^1\text{H}$  NMR and the deuterated solvent signal for  $^{13}\text{C}$  NMR as internal standards. Melting points were determined using a capillary melting point apparatus and are uncorrected. The high-resolution mass spectra (HRMS) were obtained on an Agilent Technologies Q-TOF 6520 spectrometer via electrospray ionization (ESI). The mass spectrum of **PHb-CN** was recorded on a Thermo-Scientific LCQ Fleet™ ion-trap mass spectrometer using positive ion mode ESI and a direct inlet system. The UV-vis absorption and fluorescence spectra were recorded at room temperature (approximately 20 °C) on Varian Cary 100 and Cary Eclipse spectrophotometers, respectively (both are Agilent Technologies devices) using quartz cuvettes with a path length of 1 cm. For fluorescence measurements, both the excitation and emission slit widths were 5 nm.

#### Synthesis and characterization of **Pha-e** and **PHb-CN**

The chemodosimeters **Pha-e** were synthesized in good yields (75–88%) by the Knoevenagel reaction between the appropriate 4-formylpyrazole **1a-e** and the indolium salt **2** (Scheme 2). The detailed synthetic route of **Pha-e** starting from freshly synthesized 2-hydrazinylpyridine (**4**)<sup>[20]</sup> and commercial acetophenones **3a-e** is shown in the SI† (Scheme S1). The experimental results and structural characterization data of the precursors **5a-c** and **1a-c** are consistent with our recently reported data,<sup>[9]</sup> while the results for the novel precursors **5d-e** and **1d-e** are detailed in the SI†. The structures of **Pha-e** and precursors (**1** and **5**) were elucidated by  $^1\text{H}$  and  $^{13}\text{C}$  NMR spectroscopy (Figs. S2–S11, SI†) and HRMS analysis (Figs. S12–S22, SI†). Thermogravimetric analysis (TGA) of **Pha-e** indicated that these salts exhibit high thermal stability and low solvent residues (Figs. S1, SI†).

**General procedure for the synthesis of the integrated pyrazole-hemicyanine systems **Pha-e**:** A mixture of **1a-e** (0.50 mmol), freshly synthesized 1-ethyl-2,3,3-trimethyl-3H-indol-1-ium iodide (**2**)<sup>[30]</sup> (2, 205 mg, 0.65 mmol) and sodium acetate (53 mg, 0.65 mmol) in acetic anhydride (2.0 mL) was refluxed for 3 h. Subsequently, the reaction was allowed to cool to room temperature and was concentrated under reduced pressure, and the solid residue was directly purified by flash chromatography on silica gel (eluent,  $\text{CH}_2\text{Cl}_2$ ) to afford the pure products **Pha-e** in good yields as red-orange solids.

**(E)-1-Ethyl-3,3-dimethyl-2-(2-(3-phenyl-1-(pyridin-2-yl)-1H-pyrazol-4-yl)vinyl)-3H-indolium iodide (PHa):** By following the general procedure in the reaction with 3-(phenyl-1-(pyridin-2-yl)-1H-pyrazole-4-carbaldehyde (**1a**, 125 mg, 0.5 mmol), the salt **PHa** was obtained as an orange solid (205 mg, 75%): Mp 245–244 °C.  $^1\text{H}$  NMR (400 MHz,  $\text{CDCl}_3$ ):  $\delta = 1.59$  (t,  $J = 7.1$  Hz, 3H), 1.72 (s, 6H), 4.98 (m, 2H), 7.31 (t,  $J = 5.7$  Hz, 1H), 7.49–7.57 (m, 7H), 7.68 (d,  $J = 7.0$ , 2H), 7.91 (t,  $J = 7.0$  Hz, 1H), 7.98 (d,  $J = 16.0$  Hz, 1H), 8.20 (d,  $J = 16.0$  Hz, 1H), 8.26 (d,  $J = 8.3$  Hz, 1H), 8.60 (d,  $J = 4.1$  Hz, 1H), 10.38 (s, 1H) ppm;  $^{13}\text{C}\{^1\text{H}\}$  NMR (100 MHz,  $\text{CDCl}_3$ ):  $\delta = 14.2$  (CH<sub>3</sub>), 27.4 (CH<sub>3</sub>), 44.1 (CH<sub>2</sub>), 51.9 (C), 111.8 (CH), 113.8 (CH), 114.5 (CH), 118.9 (C), 122.6 (CH), 123.1 (CH), 129.0 (CH), 129.1 (CH), 129.4 (CH), 129.6 (CH), 129.7 (CH), 131.3 (C), 132.8 (CH), 139.0 (CH), 140.3 (C), 142.9 (C), 146.5 (CH), 150.1 (C), 156.0 (C), 181.0 (C) ppm. HRMS (ESI+): calcd. For  $\text{C}_{28}\text{H}_{27}\text{N}_4^+$  419.2236 [M – I]<sup>+</sup>; found 419.2244

**(E)-1-Ethyl-3,3-dimethyl-2-(2-(3-(4-methoxyphenyl)-1-(pyridin-2-yl)-1H-pyrazol-4-yl)vinyl)-3H-indolium iodide (PHb):** By following the general procedure in the reaction with 3-(4-methoxyphenyl)-1-(pyridin-2-yl)-1H-pyrazole-4-carbaldehyde (**1b**, 140 mg, 0.5 mmol), the salt **PHb** was obtained as a red solid (214 mg, 77%): Mp 160–161 °C.  $^1\text{H}$  NMR (400 MHz,  $\text{CDCl}_3$ ):  $\delta = 1.59$  (t,  $J = 7.0$  Hz, 3H), 1.73 (s, 6H), 3.91 (s, 3H), 4.98 (m, 2H), 7.09 (d,  $J = 8.4$  Hz, 2H), 7.31 (t,  $J = 6.2$  Hz, 1H), 7.51–7.64 (m, 6H), 7.90 (t,  $J = 7.5$  Hz, 1H), 7.97 (d,  $J = 16.0$  Hz, 1H), 8.20 (d,  $J = 16.0$  Hz, 1H), 8.25 (d,  $J = 4.5$  Hz, 1H), 8.59 (s, 1H), 10.33 (s, 1H) ppm;  $^{13}\text{C}\{^1\text{H}\}$  NMR (100 MHz,  $\text{CDCl}_3$ ):  $\delta = 14.2$  (CH<sub>3</sub>), 27.4 (CH<sub>3</sub>), 44.0 (CH<sub>2</sub>), 51.8 (C), 55.5 (CH<sub>3</sub>), 111.6 (CH), 113.9 (CH), 114.3 (CH), 114.5 (CH), 119.0 (C), 122.6 (CH), 123.1 (CH), 123.6 (C), 129.3 (CH), 129.7 (CH), 130.4 (CH), 132.9 (CH), 139.0 (CH), 140.4 (C), 142.9 (C), 146.9 (CH), 149.0 (CH), 150.2 (C), 156.0 (C), 160.8 (C), 181.3 (C) ppm. HRMS (ESI+): calcd. For  $\text{C}_{29}\text{H}_{29}\text{N}_4\text{O}^+$  449.2336 [M – I]<sup>+</sup>; found 449.2332.

**(E)-1-Ethyl-3,3-dimethyl-2-(2-(3-(3,4,5-trimethoxyphenyl)-1-(pyridin-2-yl)-1H-pyrazol-4-yl)vinyl)-3H-indolium iodide (PHc):** By following the general procedure in the reaction with 3-(3,4,5-trimethoxyphenyl)-1-(pyridin-2-yl)-1H-pyrazole-4-carbaldehyde (**1c**, 170 mg, 0.5 mmol), the salt **PHc** was obtained as a red solid (264 mg, 83%): Mp 150–151 °C.  $^1\text{H}$  NMR (400 MHz,  $\text{CDCl}_3$ ):  $\delta = 1.61$  (br

m, 3H), 1.74 (s, 6H), 3.93 (br s, 9H), 4.99 (br m, 2H), 6.87 (s, 2H), 7.32 (br m, 1H), 7.52–7.57 (br m, 4H), 7.91–8.00 (br m, 2H), 8.18–8.27 (br m, 2H), 8.60 (br s, 1H), 10.35 (s, 1H) ppm;  $^{13}\text{C}\{^1\text{H}\}$  NMR (100 MHz,  $\text{CDCl}_3$ ):  $\delta = 14.2$  (CH<sub>3</sub>), 27.4 (CH<sub>3</sub>), 44.2 (CH<sub>2</sub>), 51.9 (C), 56.9 (CH<sub>3</sub>), 61.1 (CH<sub>3</sub>), 106.4 (CH), 112.0 (CH), 114.1 (CH), 114.3 (CH), 119.1 (C), 122.7 (CH), 123.3 (CH), 126.8 (C), 129.4 (CH), 129.8 (CH), 133.2 (CH), 139.1 (CH), 139.6 (C), 140.5 (C), 143.0 (C), 146.7 (CH), 149.1 (CH), 150.2 (C), 153.9 (C), 156.3 (C), 181.0 (C) ppm. HRMS (ESI+): calcd. For  $\text{C}_{31}\text{H}_{33}\text{N}_4\text{O}_3^+$  509.2547 [M – I]<sup>+</sup>; found 509.2556.

**(E)-1-Ethyl-3,3-dimethyl-2-(2-(3-(2-hydroxyphenyl)-1-(pyridin-2-yl)-1H-pyrazol-4-yl)vinyl)-3H-indolium iodide (PHd):** By following the general procedure in the reaction with 3-(2-hydroxyphenyl)-1-(pyridin-2-yl)-1H-pyrazole-4-carbaldehyde (**1d**, 133 mg, 0.5 mmol), the salt **PHd** was obtained as a red solid (256 mg, 85%): Mp 145–146 °C.  $^1\text{H}$  NMR (400 MHz,  $\text{CDCl}_3$ ):  $\delta = 1.50$  (t,  $J = 7.1$  Hz, 3H), 1.71 (s, 6H), 2.09 (s, 3H), 4.80 (m, 2H), 7.31 (m, 2H), 7.43–7.59 (m, 7H), 7.68 (d,  $J = 15.9$ , 1H), 7.88 (t,  $J = 7.5$  Hz, 1H), 8.14 (m, 2H), 8.57 (br s, 1H), 10.27 (s, 1H) ppm;  $^{13}\text{C}\{^1\text{H}\}$  NMR (100 MHz,  $\text{CDCl}_3$ ):  $\delta = 14.0$  (CH<sub>3</sub>), 21.0 (CH<sub>3</sub>), 27.0 (CH<sub>3</sub>), 43.7 (CH<sub>2</sub>), 52.1 (C), 111.5 (CH), 113.5 (CH), 114.5 (CH), 119.6 (C), 122.7 (CH), 123.1 (CH), 123.5 (CH), 125.0 (C), 126.6 (CH), 129.5 (CH), 129.6 (CH), 131.1 (CH), 131.6 (CH), 139.0 (CH), 140.2 (C), 143.1 (C), 146.4 (CH), 148.7 (C), 148.9 (CH), 150.1 (C), 151.7 (C), 169.0 (C), 181.3 (C) ppm. HRMS (ESI+): calcd. For  $\text{C}_{30}\text{H}_{29}\text{N}_4\text{O}_2^+$  477.2285 [M – I]<sup>+</sup>; found 477.2289.

**(E)-1-Ethyl-3,3-dimethyl-2-(2-(3-(4-hydroxyphenyl)-1-(pyridin-2-yl)-1H-pyrazol-4-yl)vinyl)-3H-indolium iodide (PHe):** By following the general procedure in the reaction with 3-(4-hydroxyphenyl)-1-(pyridin-2-yl)-1H-pyrazole-4-carbaldehyde (**1e**, 133 mg, 0.5 mmol), the salt **PHe** was obtained as a red solid (266 mg, 88%): Mp 105–106 °C.  $^1\text{H}$  NMR (400 MHz,  $\text{CDCl}_3$ ):  $\delta = 1.55$  (t,  $J = 7.3$  Hz, 3H), 1.73 (s, 6H), 2.34 (s, 3H), 4.86 (m, 2H), 7.29 (m, 3H), 7.48–7.60 (m, 4H), 7.70 (d,  $J = 8.6$ , 2H), 7.18 (d,  $J = 16.2$  Hz, 1H), 7.89 (d,  $J = 8.6$  Hz, 1H), 8.20 (m, 2H), 8.54 (d,  $J = 4.8$  Hz, 1H), 10.24 (s, 1H) ppm;  $^{13}\text{C}\{^1\text{H}\}$  NMR (100 MHz,  $\text{CDCl}_3$ ):  $\delta = 14.2$  (CH<sub>3</sub>), 21.2 (CH<sub>3</sub>), 27.2 (CH<sub>3</sub>), 44.0 (CH<sub>2</sub>), 51.9 (CH<sub>3</sub>), 111.8 (CH), 113.7 (CH), 114.4 (CH), 118.8 (C), 122.4 (CH), 122.7 (CH), 123.1 (CH), 128.9 (C), 129.5 (CH), 129.7 (CH), 130.1 (CH), 132.9 (CH), 139.1 (CH), 140.2 (CH), 142.9 (C), 146.1 (C), 148.9 (CH), 150.0 (C), 151.7 (CH), 154.9 (C), 169.3 (C), 180.9 (C) ppm. HRMS (ESI+): calcd. For  $\text{C}_{30}\text{H}_{29}\text{N}_4\text{O}_2^+$  477.2285 [M – I]<sup>+</sup>; found 477.2287.

**Synthesis of (E)-1-ethyl-2-(2-(3-(4-methoxyphenyl)-1-(pyridin-2-yl)-1H-pyrazol-4-yl)vinyl)-3,3-dimethylindoline-2-carbonitrile (PHb-CN):** A solution containing **PHb** (100 mg, 0.173 mmol) and NaCN (15 mg, 0.306 mmol) in ethanol:water (10:1 v/v) was stirred at 20 °C for 10 min. The product was extracted with DCM and the organic phase was concentrated under reduced pressure to afford the pure product **PHb-CN** (81 mg, 98%) as a yellow solid. Mp 120–121 °C.  $^1\text{H}$  NMR (400 MHz,  $\text{CDCl}_3$ ):  $\delta = 1.18$  (t, 3H), 1.31 (t,  $J = 7.2$ , 3H), 1.51 (s, 3H), 3.20 (m, 2H), 3.86 (s, 3H), 6.11 (d,  $J = 16.2$ , 1H), 6.62 (d,  $J = 7.6$ , 1H), 6.83 (d,  $J = 7.7$  Hz, 1H), 7.00–7.25 (m, 6H), 7.66 (d,  $J = 8.7$ , 2H), 7.80 (t,  $J = 7.3$ , 1H), 8.08 (t,  $J = 8.1$ , 1H), 8.42 (d,  $J = 4.0$ , 1H), 8.77 (s, 1H) ppm;  $^{13}\text{C}\{^1\text{H}\}$  NMR (100 MHz,  $\text{CDCl}_3$ ):  $\delta = 14.6$  (CH<sub>3</sub>), 23.2 (CH<sub>3</sub>), 24.3 (CH<sub>3</sub>), 41.0 (CH<sub>2</sub>), 49.2 (C), 55.3 (CH<sub>3</sub>), 79.8 (C), 108.2 (CH), 112.6 (CH), 114.3 (CH), 118.3 (C), 118.4 (C), 119.7 (CH), 121.6 (CH), 121.8 (CH), 123.6 (CH), 124.9 (C), 125.2 (CH), 125.8 (CH), 128.2 (CH), 129.6 (CH), 136.3 (C), 138.2 (C), 148.0 (CH), 151.1 (C), 152.5 (C), 160.0 (C) ppm. MS (ESI)  $m/z = 476.25$  ( $\text{MH}^+$ , 10%) and 449.28 ( $\text{MH}^+ - \text{HCN}$ , 100%);  $m/z$  calcd. ( $\text{C}_{30}\text{H}_{30}\text{N}_5\text{O}^+$ ) = 476.24 [ $\text{MH}^+$ ] and 449.23 [ $\text{M} - \text{HCN}^+$ ] (Figs. S35 and S37, SI†).

#### Photophysical properties of salts **Pha-e**

**UV-vis absorption and fluorescence studies:** The solvatochromic studies of the compounds **Pha-e** were carried out in  $1.0 \times 10^{-5}$  M solutions using different solvents (Figs. S23–S27), such as toluene (PhMe), dichloromethane (DCM), acetonitrile (ACN), dimethylsulfoxide (DMSO), ethanol (EtOH), and water ( $\text{H}_2\text{O}$ ).

**Determination of quantum yields:** The quantum yields were obtained (Table S1, SI†) by using quinine sulfate ( $\phi_F = 0.50$  in  $\text{H}_2\text{SO}_4$  0.5 M at 300 nm) as a reference and calculated according to the equation<sup>[24,31]</sup>

$$\phi_{f,x} = \phi_{f,st} \cdot \frac{F_x}{F_{st}} \cdot \frac{1 - 10^{-A_{st}}}{1 - 10^{-A_x}} \cdot \frac{\eta_{st}^2}{\eta_x^2}$$

where x and st indicate the sample and standard solution, respectively,  $\phi$  is the quantum yield, F is the integrated area of the emission, A is the absorbance at the excitation wavelength, and  $\eta$  is the refraction index of solvents.

#### Design of the **Pha-e** Chemosensors

**Response detection of **Pha-e**:** The solutions of probes **Pha-e** ( $4.0 \times 10^{-5}$  M) were prepared in ethanol-water (99:1, v/v at pH = 7.05, 20 °C). The salts used in

## FULL PAPER

WILEY-VCH

the stock solutions were AcONa, BrK, NaHSO<sub>4</sub>, KNO<sub>3</sub>, NaClO<sub>3</sub>, Na<sub>2</sub>SO<sub>4</sub>, NaF, NaH<sub>2</sub>PO<sub>4</sub>, NaHSO<sub>3</sub>, NaI, NaN<sub>3</sub>, NaNO<sub>2</sub>, Na<sub>2</sub>S, NaSCN, and NaCN. These salts were dissolved in deionized water to afford the respective aqueous solutions (1.2 × 10<sup>-4</sup> M). Measurements of absorption and fluorescence emission (λ<sub>exc</sub> = 300 nm) of PHa-e were taken when adding 3 equiv of several anions to 1 equiv of probe solution, achieving EtOH:H<sub>2</sub>O final solutions (approximately 1:1 v/v). The resulting solutions were stirred and held for 5 min before taking the respective measurements, although the response (the addition reaction) was immediate when NaCN was used (Figs. 1 and S28–S32 of SI†).

**Determination of the detection limit:** The LOD of PHb and PHd (4.0 × 10<sup>-5</sup> M in EtOH) was obtained by 3σ/k, where σ is the standard deviation of the blank measurements (10 times), and k is the slope from the plot Log(A<sub>1</sub>/A<sub>2</sub>) versus [CN<sup>-</sup>] (Figs. 2 and S33–S34 of SI†).<sup>[32]</sup> The UV–vis titration of probes was evaluated after progressive addition of CN<sup>-</sup> ions (0–1 equiv dissolved in water), achieving EtOH:H<sub>2</sub>O final solutions (round 1:1 v/v).

**Preparation of yellow-test strips:** Filter paper was immersed in an ethanolic solution (1.2 × 10<sup>-4</sup> M) of the probe PHd, and dried in an oven at 40 °C for 20 min. Then, the test strips were immersed in aqueous solution containing 0.00 to 1.00 equiv of CN<sup>-</sup> ions (Fig. 3a). Likewise, the test strips were used with 3 equiv of interfering anions (OAc<sup>-</sup>, Br<sup>-</sup>, HSO<sub>4</sub><sup>-</sup>, NO<sub>3</sub><sup>-</sup>, ClO<sub>3</sub><sup>-</sup>, SO<sub>4</sub><sup>2-</sup>, F<sup>-</sup>, H<sub>2</sub>PO<sub>4</sub><sup>-</sup>, HSO<sub>3</sub><sup>-</sup>, I<sup>-</sup>, N<sub>3</sub><sup>-</sup>, NO<sub>2</sub><sup>-</sup>, S<sub>2</sub><sup>-</sup>, SCN<sup>-</sup>) in studies of both selective and competition (Fig. 3b). This method could be used for the selective CN<sup>-</sup> recognition in different water samples.

**Cyclic voltammetry and valuation of the energy band gap:** Cyclic voltammetry (CV) experiments were performed on an Autolab PGSTAT302N potentiostat. The experiment was carried out in a cell with three electrodes, an ITO working electrode, an Ag/AgCl (NaCl 3 M) reference electrode and a Pt (wire) counter electrode. The experiment was carried out using a solution 0.1 M tetrabutylammonium hexafluorophosphate (TBAPF<sub>6</sub>) in dry ACN as the support electrolyte, and analytes were prepared at a concentration of 10<sup>-4</sup> M. The analytes were used as the external standard ferrocene [Fe(Cp)<sub>2</sub>] to 10<sup>-3</sup> M. For each voltammetry, molecular nitrogen (N<sub>2</sub>) was bubbled through the solution for five minutes, and a 5 scan was performed for each voltammogram, with the potential varying from -1.0 to +2.0 V and a scan speed of 100 mV s<sup>-1</sup> (Figs. S38–S44 and Table S2, SI†).

**Theoretical calculation:** Theoretical calculations were conducted using DFT in Gaussian 09. The DFT calculations employed the B3LYP hybrid functional and the 6-311G+(d,p) basis set. The polarizable continuum model (PCM) was used to optimize the ground and excited state geometries in ACN.<sup>[33]</sup> Time-dependent (TD-DFT) calculations were performed on optimized geometries.<sup>[34]</sup> The visual software used in this work to analyze the output files performed in the calculations was Gauss View 6 (Figs. S45 and Table S3, SI†).

## Acknowledgements

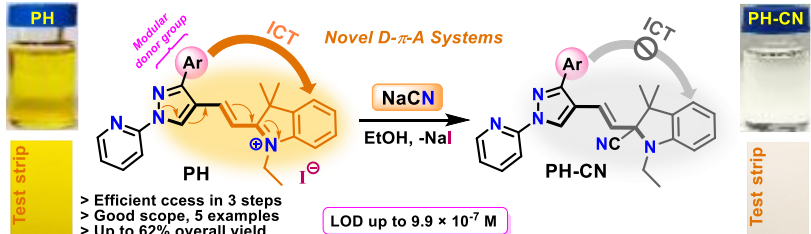
We wish to thank the Chemistry Department and Vicerrectoria de Investigaciones from Universidad de los Andes for financial support. We express our gratitude to the Colombian Institute for Science and Research (COLCIENCIAS, project code 120465843502) for financial support. We also wish to thank Diana Pinilla and Edwin Guevara (both of Universidad de los Andes) for acquiring the thermograms and mass spectra, respectively.

**Keywords:** Chemodosimeter • Charge transfer • Cyanide • Hemicyanine • N-(2-pyridyl)pyrazole

- [1] a) J. R. Askim, M. Mahmoudi, K. S. Suslick, *Chem. Soc. Rev.* **2013**, *42*, 8649–8682; b) T. L. Mako, J. M. Racicot, M. Levine, *Chem. Rev.* **2019**, *119*, 322–477.  
 [2] X. Cheng, Q. Li, C. Li, J. Qin, Z. Li, *Chem. Eur. J.* **2011**, *17*, 7276–7281.  
 [3] a) A. Brüger, G. Faflek, B. O. J. Restrepo, L. Rojas-Mendoza, *Sci. Total Environ.* **2018**, *627*, 1167–1173; b) A. E. Sánchez-Chacón, G. T. Lapidus, *Hydrometallurgy* **1997**, *44*, 1–20; c) L. Junjian, C. Zengyan, X. Pan, D. Wei, J. Ai-Qun, *Dye. Pigment.* **2019**, *168*, 175–179.  
 [4] a) R. K. Bhandari, R. P. Oda, I. Petrikovics, D. E. Thompson, M. Brenner, S. B. Mahon, *J. Anal. Toxicol.* **2014**, *38*, 218–225; b) F. J. Baud, *Human & Experimental Toxicology.* **2007**, *26*, 191–201.

- [5] W. C. Lin, J. W. Hu, K. Y. Chen, *Anal. Chim. Acta.* **2015**, *893*, 91–100.  
 [6] A. Maksim, I. Ruslan, J. Jenkins, B. Papkovsky, D. Heindl, *ACS Sens.* **2016**, *6*, 702–709.  
 [7] A. Mohammadi, S. Yaghoobi, *Sens. Actuator B-Chem.* **2017**, *241*, 1069–1075.  
 [8] a) M. Tomasulo, S. Sortino, A. J. P. White, F. M. Raymo, *J. Org. Chem.* **2006**, *71*, 744–753; b) Y. Shiraishi, S. Sumiya, T. Hiraia, *Chem. Commun.* **2011**, *47*, 4953–4955; c) K. Prakash, P. R. Sahoo, S. Kumar, *Sens. Actuator B-Chem.* **2016**, *237*, 856–864; d) S. Wen, S. Guo, H. Chong, *Chem. Rev.* **2016**, *116*, 7768–7817; e) J. Orrego-Hernández, C. Lizarazo, J. Cobo, J. Portilla, *RSC Adv.* **2019**, *9*, 27318–27323.  
 [9] J. Orrego-Hernández, J. Portilla, *J. Org. Chem.* **2017**, *82*, 13376–13385.  
 [10] A. Tigreros, H. A. Rosero, J. C. Castillo, J. Portilla, *Talanta.* **2019**, *196*, 395–401.  
 [11] a) W. Sun, J. Fan, C. Hu, J. Cao, H. Zhang, X. Xiong, J. Wang, S. Cui, S. Suna, X. Peng, *Chem. Commun.* **2013**, *49*, 3890–3892; b) H. A. Shindy, *Dye. Pigment.* **2018**, *149*, 783–788.  
 [12] A. Mishra, R. K. Behera, P. K. Behera, B. K. Mishra, G. B. Behera, *A Review, Chem. Rev.* **2000**, *100*, 1973–2012.  
 [13] a) V. Polishchuk, M. Stanko, A. Kulinich, M. Shandura, *Eur. J. Org. Chem.* **2018**, 240–246; b) H. Chen, M. S. Farahat, K. Law, D. G. Whitten, *J. Am. Chem. Soc.* **1996**, *118*, 2584–2594; c) S. M. Usama, T. Thompson, K. Burgess, *Angew. Chem.* **2019**, *58*, 8974–8976.  
 [14] S. Zhang, H. Zhu, J. Huang, L. Kong, Y. Tian, J. Yang, *ChemistrySelect.* **2019**, *4*, 7380–7387.  
 [15] A. Hagfeldt, G. Boschloo, L. Sun, L. Kloo, H. Pettersson, *Chem. Rev.* **2010**, *110*, 6595–6663.  
 [16] S. Chidirala, H. Ulla, A. Valaboju, M. R. Kiran, M. E. Mohanty, M. N. Satyanarayan, G. Umesh, K. Bhanuprakash, V. J. Rao, *J. Org. Chem.* **2016**, *812*, 603–614.  
 [17] a) S. Wanga, X. Feia, J. Guo, Q. Yang, Y. Li, Y. Song, *Talanta.* **2016**, *148*, 229–236; b) R. Kaushik, A. Ghosh, A. Singh, P. Gupta, A. Mittal, D. A. Jose, *ACS Sens.* **2016**, *10*, 1265–1271; c) Y. Li, J. Chen, T. S. Chu, *J. Lumin.* **2016**, *179*, 203–210; d) J. C. Castillo, A. Tigreros, J. Portilla, *J. Org. Chem.* **2018**, *83*, 10887–10897; e) J. C. Castillo, J. Portilla, *Targets Heterocycl. Syst.* **2018**, *22*, 194–223.  
 [18] a) B. Willy, T. J. J. Müller, *Org. Lett.* **2011**, *13*, 2082–2085; b) S. K. Lanke, N. Sekar, *Dye. Pigment.* **2016**, *127*, 116–127; c) X. Q. Wei, G. Yang, J. B. Cheng, Z. Y. Lu, M. G. Xie, *Opt. Mater.* **2007**, *29*, 936–940.  
 [19] a) J. Orrego-Hernández, N. Nuñez-Dallos, J. Portilla, *Talanta.* **2016**, *152*, 432–437; b) M. García, I. Romero, J. Portilla, *ACS Omega.* **2019**, *4*, 6757–6768.  
 [20] J. Orrego-Hernández, J. Cobo, J. Portilla, *Eur. J. Org. Chem.* **2015**, 5064–5069.  
 [21] X. Peng, F. Song, E. Lu, Y. Wang, W. Zhou, J. Fan, Y. Gao, *J. Am. Chem. Soc.* **2005**, *127*, 4170–4171.  
 [22] H. H. Jaffe, *Chem. Rev.* **1953**, *53*, 191–261.  
 [23] W. West, S. Pearce, *J. Phys. Chem.* **1965**, *69*, 1894–1903.  
 [24] C. Würth, M. Grabolle, J. Pauli, M. Spieles, U. Resch-genger, *Nat. Protoc.* **2013**, *8*, 1535–1550.  
 [25] P. Mehta, G. Hwang, J. Park, K. H. Lee, *Anal. Chem.* **2018**, *90*, 11256–11264.  
 [26] J. R. Lenhard, R. L. Parton, *J. Am. Chem. Soc.* **1987**, *109*, 5808–5813.  
 [27] J. R. Lenhard, A. D. Cameron, *J. Phys. Chem.* **1993**, *97*, 4916–4925.  
 [28] Y. Xiao, G. Han, J. Wu, J. Y. Lin, *J. Power Sources.* **2016**, *306*, 171–177.  
 [29] C. Kanth, J. Patel, M. Chauhan, M. Aatif, A. Sharma, M. U. Trivedi, B. Tripathi, P. Tiwari, G. Gupta, M. Kumar, M. Kumar-Pandey, *New J. Chem.* **2017**, *41*, 5836–5845.  
 [30] E. A. Owens, N. Bruschi, J. G. Tawney, M. Henary, *Dyes Pigm.* **2015**, *113*, 27–37.  
 [31] a) A. M. Brouwer, *Pure Appl. Chem.* **2011**, *83*, 2213–2228; b) A. N. Fletcher, *Photochem. Photobiol.* **1969**, *9*, 439–444.  
 [32] G. L. Long, J. D. Winefordner, *Anal. Chem.* **1983**, *55*, 712A–724A.  
 [33] M. Cossi, N. Rega, G. Scalmani, V. Barone, *J. Comput. Chem.* **2003**, *24*, 669–681.  
 [34] A. Becke, *J. Chem. Phys.* **1993**, *98*, 5648–5652.

## Entry for the Table of Contents

FULL PAPER	
 <p> <b>PH</b>            Test strip            &gt; Efficient ccess in 3 steps            &gt; Good scope, 5 examples            &gt; Up to 62% overall yield  <b>LOD up to <math>9.9 \times 10^{-7}</math> M</b> </p> <p> <b>PH-CN</b>            Test strip         </p> <p>           Novel D-<math>\pi</math>-A Systems            NaCN            EtOH, -NaI         </p>	<p><b>Key Topic*</b></p> <p>* Hemicyanine-functionalized N-(2-pyridyl)pyrazoles, cyanide sensing</p> <p>Luz-Mery Garzón and Jaime Portilla*</p> <p><b>Page No. – Page No.</b></p> <p><b>Title</b> Synthesis of novel D-<math>\pi</math>-A dyes for colorimetric cyanide sensing based on hemicyanine-functionalized N-(2-pyridyl)pyrazoles</p>
<p>Herein, a novel family of D-<math>\pi</math>-A organic dyes for colorimetric cyanide sensing based on hemicyanine-functionalized N-(2-pyridyl)pyrazoles are provided. These dyes displayed high selectivity and sensitivity for CN<sup>-</sup> (LOD of up to <math>9.9 \times 10^{-7}</math> M) by interrupting the D-<math>\pi</math>-A system by nucleophilic attack of the anion on the iminium group of the dyes.</p>	